

MARTIN MARIETTA ENERGY SYSTEMS LIBRARIES



3 4456 0353216 7

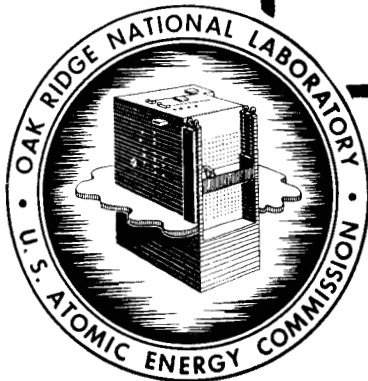
ORNL-1496
Progress

4a

PHYSICS DIVISION
QUARTERLY PROGRESS REPORT
FOR PERIOD ENDING DECEMBER 20, 1952

CENTRAL RESEARCH LIBRARY
DOCUMENT COLLECTION
LIBRARY LOAN COPY
DO NOT TRANSFER TO ANOTHER PERSON

If you wish someone else to see this document,
send in name with document and the library will
arrange a loan.



OAK RIDGE NATIONAL LABORATORY
OPERATED BY
CARBIDE AND CARBON CHEMICALS COMPANY
A DIVISION OF UNION CARBIDE AND CARBON CORPORATION



POST OFFICE BOX P
OAK RIDGE, TENNESSEE

ORNL-1496

This document consists of 29 pages.
Copy 4 of 332 copies. Series A.

Contract No. W-7405-eng-26

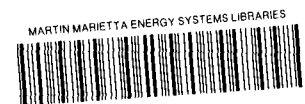
PHYSICS DIVISION
QUARTERLY PROGRESS REPORT
for Period Ending December 20, 1952

A. H. Snell, Director
E. O. Wollan, Associate Director

DATE ISSUED

MAR 1 1953

OAK RIDGE NATIONAL LABORATORY
Operated by
CARBIDE AND CARBON CHEMICALS COMPANY
A Division of Union Carbide and Carbon Corporation
Post Office Box P
Oak Ridge, Tennessee



3 4456 0353216 7

ORNL-1496

This document consists of 29 pages.
Copy of 332 copies. Series A.

Contract No. W-7405-eng-26

PHYSICS DIVISION
QUARTERLY PROGRESS REPORT
for Period Ending December 20, 1952

A. H. Snell, Director
E. O. Wollan, Associate Director

DATE ISSUED

OAK RIDGE NATIONAL LABORATORY
Operated by
CARBIDE AND CARBON CHEMICALS COMPANY
A Division of Union Carbide and Carbon Corporation
Post Office Box P
Oak Ridge, Tennessee



INTERNAL DISTRIBUTION

- | | | | |
|-------|---|-----|-------------------------------|
| 1. | C. E. Center | 36. | E. P. Blizzard |
| 2. | Biology Library | 37. | M. E. Rose |
| 3. | Health Physics Library | 38. | G. E. Boyd |
| 4-5. | Central Research Library | 39. | Lewis Nelson |
| 6. | Reactor Experimental
Engineering Library | 40. | R. W. Stoughton |
| 7-12. | Central Files | 41. | C. E. Winters |
| 13. | C. E. Larson | 42. | W. H. Jordan |
| 14. | W. B. Humes (K-25) | 43. | E. C. Campbell |
| 15. | L. B. Emler (Y-12) | 44. | D. S. Billington |
| 16. | A. M. Weinberg | 45. | M. A. Bredig |
| 17. | E. H. Taylor | 46. | R. S. Livingston |
| 18. | E. D. Shipley | 47. | C. P. Keim |
| 19. | E. J. Murphy | 48. | J. L. Meem |
| 20. | F. C. VonderLage | 49. | C. E. Clifford |
| 21. | A. H. Snell | 50. | G. H. Clewett |
| 22. | J. A. Swartout | 51. | C. D. Susano |
| 23. | A. Hollaender | 52. | C. J. Borkowski |
| 24. | K. Z. Morgan | 53. | M. J. Skinner |
| 25. | F. L. Steahly | 54. | L. A. Rayburn |
| 26. | M. T. Kelley | 55. | S. Bernstein |
| 27. | E. M. King | 56. | P. M. Reyling |
| 28. | E. O. Wollan | 57. | D. D. Cowen |
| 29. | D. W. Cardwell | 58. | W. M. Good |
| 30. | A. S. Householder | 59. | G. C. Williams |
| 31. | L. D. Roberts | 60. | J. L. Fowler |
| 32. | R. B. Briggs | 61. | E. P. Wigner (consultant) |
| 33. | R. N. Lyon | 62. | H. A. Bethe (consultant) |
| 34. | W. C. Koehler | 63. | K. Lark-Horovitz (consultant) |
| 35. | W. K. Ergen | 64. | Eugene Guth (consultant) |
| | | 65. | J. G. Daunt (consultant) |

EXTERNAL DISTRIBUTION

- 66. L. C. Biedenharn, Sloans Physics Laboratory
- 67. R. F. Bacher, California Institute of Technology
- 68-69. Ohio State University, Attn: Professor of Naval Science
- 70. John Dunning, Columbia University
- 71. Phillips Petroleum Co., Attn: Librarian
- 72. R. L. Heath, American Cyanamid Co.
- 73. S. DeBenedetti, Carnegie Institute of Technology
- 74. Massachusetts Institute of Technology, Department of
Electrical Engineering
- 75. A. von Hippel, Laboratory for Insulation Research, MIT
- 76. M. Goodrich, Louisiana State University
- 77. Truman S. Grey
- 78-332. Given distribution as shown in TID 4500 under Physics Category

Physics Division quarterly progress reports previously issued in this series are as follows:

ORNL-325 Supplement	December, January, and February, 1948-1949
ORNL-366	Period Ending June 15, 1949
ORNL-481	Period Ending September 25, 1949
ORNL-577	Period Ending December 15, 1949
ORNL-694	Period Ending March 15, 1950
ORNL-782	Period Ending June 15, 1950
ORNL-865	Period Ending September 20, 1950
ORNL-940	Period Ending December 20, 1950
ORNL-1005	Period Ending March 20, 1951
ORNL-1092	Period Ending June 20, 1951
ORNL-1164	Period Ending September 20, 1951
ORNL-1278	Period Ending December 20, 1951
ORNL-1289	Period Ending March 20, 1952
ORNL-1365	Period Ending June 20, 1952
ORNL-1415	Period Ending September 20, 1952

CONTENTS

	PAGE
PUBLICATIONS	vi
ANNOUNCEMENTS	vi
SUMMARY	1
1. HIGH-VOLTAGE PHYSICS	2
Reactions with the Cockcroft-Walton He ³ Beam	2
The He ³ + Li ⁷ reactions	2
The He ³ + H ³ reactions	3
Angular Distribution of Neutrons Scattered from Nitrogen	4
2. RADIOACTIVITY AND NUCLEAR ISOMERISM	7
Coincidence Spectroscopy of Gamma Rays from Ta ¹⁸¹	7
Os ¹⁹¹ to Ir ¹⁹¹ Decay Scheme	8
Angular Correlation of Gamma Rays	8
Chemical Separation of 0.82-sec Pb ^{207m} from Bi ²⁰⁷	8
Tritium-Produced Activities in Neutron-Irradiated Lithium Compounds	9
3. NEUTRON DIFFRACTION	10
Neutron-Diffraction Studies of Binary Ferromagnetic Alloys	10
Magnetic Scattering of Neutrons by Neodymium and Erbium	12
4. NEUTRON CROSS SECTIONS AND NEUTRON DECAY	14
Time-of-Flight Spectrometer Studies	14
Nickel	14
Nickel-62	14
Neutron Decay	14
5. HEAVY-ION PHYSICS	17
Equipment and Techniques	17
6. THEORETICAL PHYSICS	20
Production of Polarized Particles in Nuclear Reactions	20
Quantum Electrodynamics	21
Magnetic Scattering of Slow Neutrons by Atoms with Nonzero Orbital Angular Momentum	22
Effect of Finite DeBroglie Wave Length in Beta Decay	22

PUBLICATIONS

The following papers by members of the Physics Division appeared in open publications during the last quarter:

R. W. Lamphere and G. P. Robinson, "A Converted Electron Accelerator to Produce 2.3-Mev Positive Ions," *Nucleonics* **10**, No. 10, 28 (1952).

J. L. Fowler, W. H. Jones, and J. H. Paehler, "Fission Asymmetry as a Function of Excitation Energy of the Compound Nucleus," *Phys. Rev.* **88**, 71 (1952).

H. Pomerance, "Thermal Neutron Capture Cross Sections," *Phys. Rev.* **88**, 412 (1952).

L. C. Biedenharn, K. Boyer, and R. A. Charpie, "Angular Correlations of the Radiations from Deuteron Stripping Reactions," *Phys. Rev.* **88**, 517 (1952).

J. M. Blatt and L. C. Biedenharn, "The Angular Distribution of Scattering and Reaction Cross Sections," *Revs. Mod. Phys.* **24**, 258 (1952).

L. C. Biedenharn, J. M. Blatt, and M. E. Rose, "Some Properties of the Racah and Associated Coefficients," *Revs. Mod. Phys.* **24**, 249 (1952).

A. H. Snell, "The Nuclear Reactor as a Research Implement," *Am. J. Phys.* **20**, 527 (1952).

ANNOUNCEMENTS

The following persons have been added to the staff of the Physics Division during this quarter: E. D. Klema and C. C. Harris (transferred from ORSORT to Scintillation Spectrometry group); L. W. Gilley and J. H. Marable (ANP Critical Experiments).

PHYSICS DIVISION QUARTERLY PROGRESS REPORT

SUMMARY

High-Voltage Physics. The 2-Mev Van de Graaff has been put into successful operation in the new permanent High-Voltage Building, and the 5-Mev Van de Graaff has been moved from Y-12 and installed in the High-Voltage Building during this period.

The angular distributions of neutrons elastically scattered by nitrogen at the resonance energies of 1.35, 1.40, 1.60, 1.78, and 2.25 Mev have been investigated.

Helium-3 accelerated with the Cockcroft-Walton machine has been used to bombard Li^7 and H^3 . The resultant modes of disintegrations of the excited B^{10} in the first case and Li^6 in the second case have been studied with a scintillation spectrometer. The cross sections of three reactions resulting from He^3 bombardment of H^3 are given as a function of energy.

Radioactivity and Nuclear Isomerism. The gamma-ray transitions of 132 and 135 keV in Ta^{181} and 128 keV in Ir^{191} are classified from measurements of the K-shell internal conversion coefficients.

Measurement of the angular correlation of the gamma-ray cascade in Ni^{60} has been completed, and further work is reported on the angular correlation of gamma-ray cascades in Ta^{181} .

The 0.82-sec isomer of Pb^{207} has been separated from Bi^{207} by ion exchange, which establishes for the first time the genetic relationship by direct observation of the decay of the short-period activity after chemical separation.

Evidence is presented for the production of the $\text{Li}^6(t,p)\text{Li}^8$ and $\text{F}^{19}(t,p)\text{F}^{21}$ reactions by fast tritons obtained from neutron-irradiated lithium compounds enriched in Li^6 .

Neutron Diffraction. Neutron-diffraction studies have been made on the binary alloys, Ni_3Fe , FeCo , and Ni_3Mn . The studies were made for both the ordered and disordered states, and the results have been combined with magnetic-saturation data to give the magnetic moments of the atoms in these alloys.

The two rare earths, neodymium and erbium, have been investigated by the neutron-diffraction technique over the temperature range of 300 to 4°K. Neodymium showed only the diffuse scattering characteristic of paramagnetism, whereas erbium was found to be ferromagnetic below the temperature of liquid nitrogen. A change in the magnetic properties was observed below the temperature of liquid hydrogen.

Neutron Cross Sections and Neutron Decay. A resonance at 4200 eV has been observed for the separated isotope, Ni^{62} , by use of the time-of-flight spectrometer.

An attempt was made to measure the momentum spectrum of the recoil protons associated with the decay of the neutron. The flux at the LITR was insufficient to obtain conclusive results, and it is proposed to carry out the experiment at the MTR. Preliminary measurements are now being made with the decay of He^6 .

Heavy-Ion Physics. A discussion is given of some points pertinent to the analysis of data relating to the distribution in space of ionization produced by a beam of heavy ions entering a gas.

Theoretical Physics. Previously reported work on the magnetic scattering of slow neutrons by nonzero orbital atomic moments has been extended, but without numerical results as yet. A general formula has been derived for

HIGH-VOLTAGE PHYSICS

the polarization of the products of nuclear reactions, with the result that the experimental production of intense polarized fast neutron and proton beams seems to be a rather simple task. Finally, previous work on quantum electrodynamics has been extended, and preliminary, improved results for the level shift in hydrogen are given.

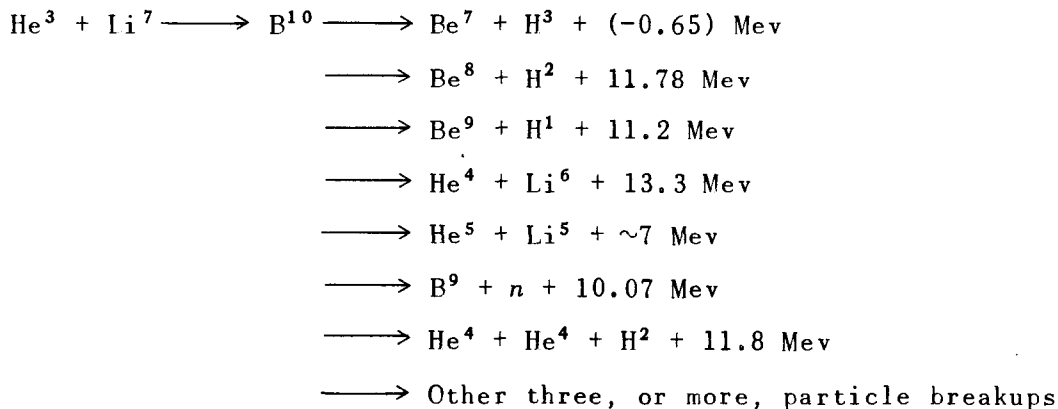
In order to facilitate analyses of forbidden beta spectra, extensive numerical calculations of the relevant parts of the correction factors were undertaken some time ago. The calculations are now finished, and as a result of this work it appears that the procedure for constructing Kurie plots of both allowed and forbidden spectra should be revised somewhat.

1. HIGH-VOLTAGE PHYSICS

REACTIONS WITH THE COCKCROFT-WALTON He³ BEAM

W. M. Good C. D. Moak
W. E. Kunz

The He³ + Li⁷ Reactions. It has been possible, by means of a ten-channel pulse analyzer, to identify some of the modes of decay of B¹⁰ excited to 17.2 Mev by the capture of He³ on Li⁷. At this energy level, excitation B¹⁰ breaks up in the following ways:



A 3-mil aluminum absorber serves to prevent alpha particles from entering the scintillation spectrometer and thus permits observation of the spectrum of protons and deuterons in these reactions. Figure 1.1 shows the pulse spectrum obtained. The 3-mil aluminum absorber reduces the energies

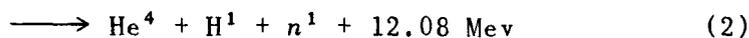
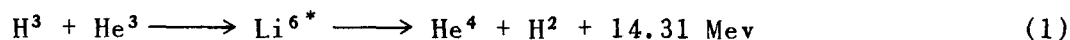
it can be interpreted as exhibiting, within the accuracy of the experiment, the groups of protons and deuterons just mentioned. The conclusion at present is that B¹⁰ at 17.2-Mev excitation breaks up into both Be⁸ and Be⁹ and each of these to its first excited state, as well as to its

ground state. Since the pertinent nuclear masses are known to some tens of kilovolts, the proton group that corresponds to Be^9 in its ground state will serve as a spectrometer calibration. More study will be required to establish other than two groups of protons and two groups of deuterons.

The $\text{He}^3 + \text{H}^3$ Reactions. The following are the reactions that have been studied:

In the case of reaction 3, the ground state of He^5 has been observed as a peak in the proton spectrum. By using the scintillation spectrometer described in the last quarterly report,⁽¹⁾ the energy of this peak has been found to lie at 9.38 ± 0.05 Mev. From this result, the energy of breakup

⁽¹⁾ W. M. Good, W. E. Kunz, and C. D. Moak, *Phys. Quar. Prog. Rep. Sept. 20, 1952, ORNL-1415, p. 4.*



UNCLASSIFIED
DWG. 18071

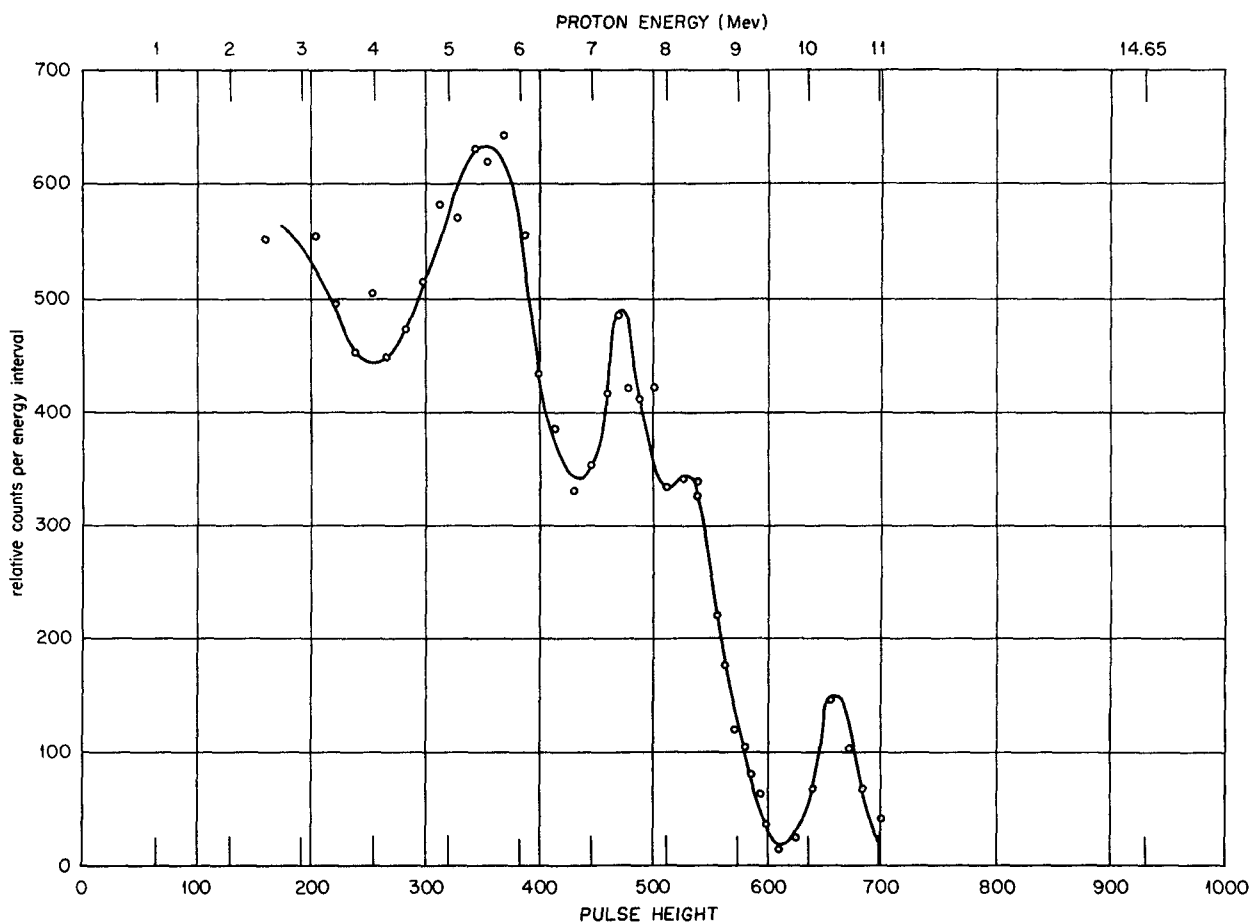


Fig. 1.1. Pulse Spectrum in Sodium Iodide Produced by Protons and Deuterons from Decay Products of B^{10} Excited to 17.2 Mev by $\text{He}^3 + \text{Li}^7$.

HIGH-VOLTAGE PHYSICS

of He^5 into a neutron and an alpha particle is found to be 0.95 ± 0.07 Mev, which gives a value of 5.01388 ± 0.00007 atomic mass units for He^5 .

In the case of reaction 1, the deuterons have been found to be emitted isotropically with respect to the incident He^3 ion beam at a bombarding energy of 360 kev.

In the case of reaction 2, the spectrum of protons from the three-body mode of breakup, as indicated in Fig. 1.2, is not that which would be predicted from simple statistical mechanical arguments (see Fig. 1.3).

Competitions among the modes of decay 1, 2, and 3 do not vary with bombarding energy (within 20% limits of experimental uncertainty) in the 225- to 600-kev range.

The cross section for reactions 1, 2, and 3 is shown in Fig. 1.4. The target employed was less than 20 kev

thick throughout the range of bombarding energies used. The shape of the curve has been compared with the shapes of Coulomb penetrability curves calculated for various values of the radius of interaction for *S*-wave and *P*-wave penetration (see Figs. 1.5 and 1.6). The data seem to fit the shape of *S*-wave penetrability curves much more closely than those for *P*-wave penetrability, which, in addition to the isotropy of the deuterons, suggests but does not prove the existence of a level in Li^6 with $J = 1$, even parity.

ANGULAR DISTRIBUTION OF NEUTRONS SCATTERED FROM NITROGEN

J. L. Fowler C. H. Johnson

Angular distribution of elastic scattering of neutrons by nitrogen at energies corresponding to resonances in the total cross section has been

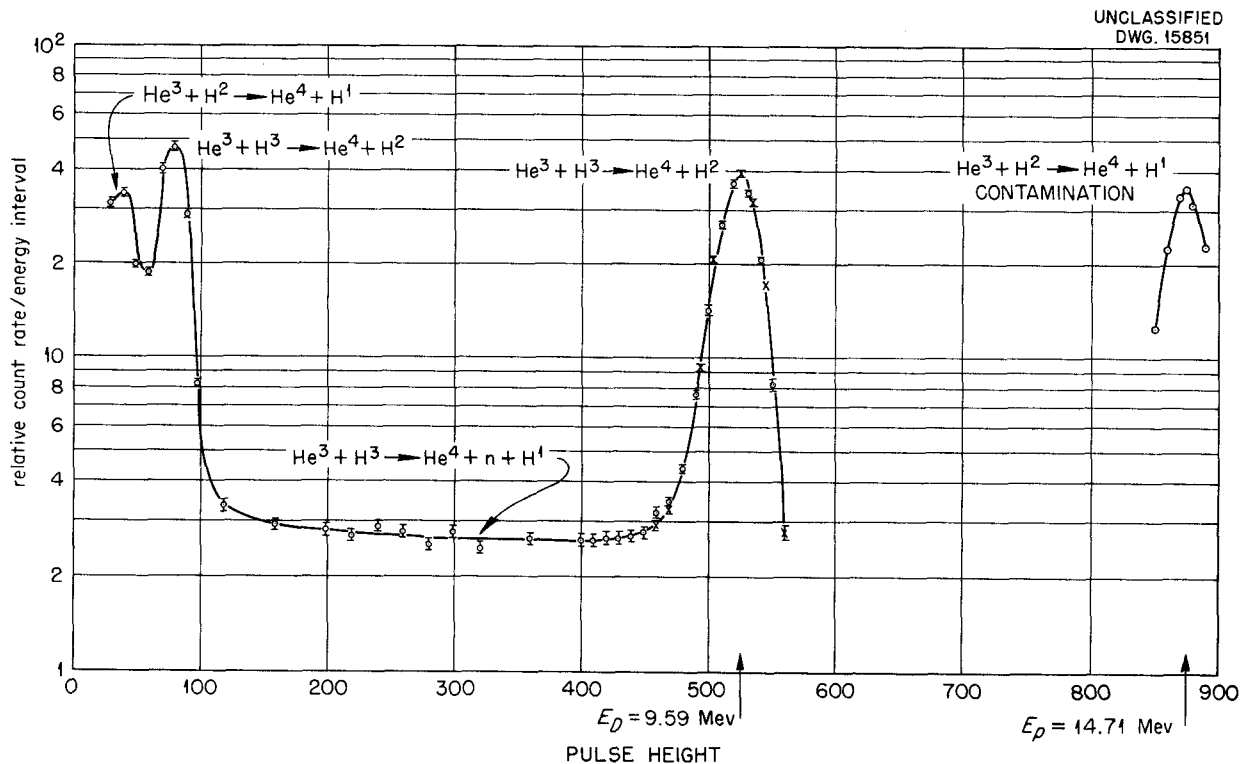


Fig. 1.2. Pulse Spectrum in Sodium Iodide of Particles from $\text{He}^3 + \text{H}^3$ (Bombarding Energy, 300 kev).

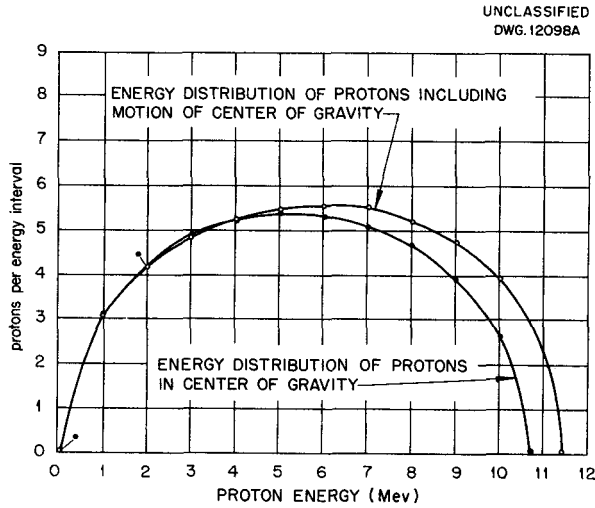


Fig. 1.3. Energy Distribution of Protons.

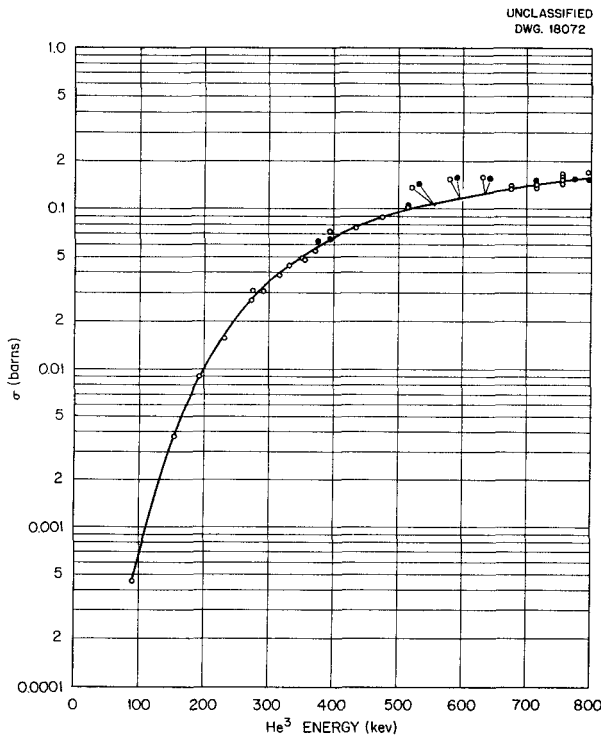
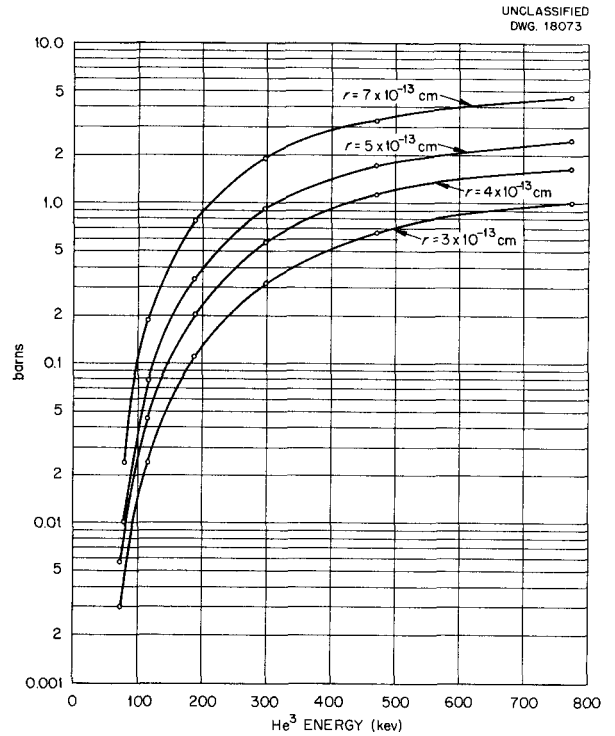


Fig. 1.4. Total Cross Section for the $H^3(He^3, d)He^4$, $H^3(He^3, p)He^5$, and $H^3(He^3, p)He^4, n^1$ Reactions.



S-Wave Penetration for $H^3 + He^3$ Without Statistical Weight Factor ($8\pi\chi r P_0$)

Fig. 1.5. S-Wave Penetration for $H^3 + He^3$ Without Statistical Weight Factor ($8\pi\chi r P_0$).

investigated by the method of pulse-height analysis of nitrogen recoil energy.⁽²⁾ The resonances at 1.350, 1.40, 1.60, 1.78, and 2.25 Mev^(3,4) have been studied.

Neutrons were produced by bombarding a tritium gas target with protons from the 5-Mev Van de Graaff. The nitrogen recoil counter was placed with its axis at zero degrees to the proton beam. In order to determine the average energy of the neutrons entering the nitrogen chamber, the number of nitrogen recoils counted with a low integral bias was measured

(2) J. L. Fowler, C. H. Johnson, and J. R. Risser, *Phys. Quar. Prog. Rep. Sept. 20, 1952*, ORNL-1415, p. 2.

(3) J. J. Hinchley, P. H. Stelson, and W. M. Preston, *Phys. Rev. 86*, 483 (1952).

(4) C. H. Johnson, H. B. Willard, J. K. Blair, and J. D. Kingston, *Phys. Quar. Prog. Rep. June 20, 1952*, ORNL-1365, p. 1.

HIGH-VOLTAGE PHYSICS

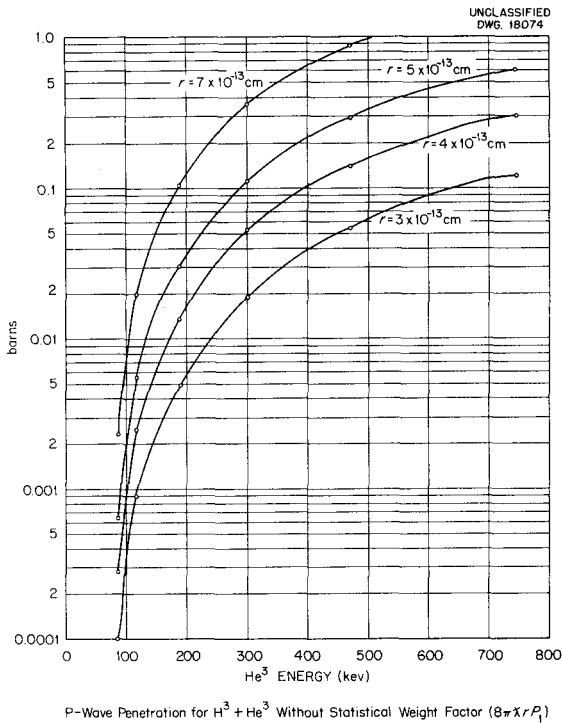


Fig. 1.6. P-Wave Penetration for $H^3 + He^3$ Without Statistical Weight Factor ($8\pi\chi r P_1$).

as a function of the current in the proton magnetic analyzer. The peaks of the curve observed in this manner correspond in energy to the known neutron resonance energies.^(3,4) In obtaining and using this calibration, errors resulting from hysteresis in the analyzing magnet were minimized by always increasing the magnet current during a run; furthermore, in using this calibration, any systematic shift was removed by redetermining the calibration point just below the neutron energy to be used. The experimental widths of the resonances observed in the calibration process, corrected for the known natural widths of the resonances,⁽³⁾ indicated that the neutron energy resolution was about 20 keV (full width at half maximum).

Figure 1.7 shows two typical angular distribution curves for

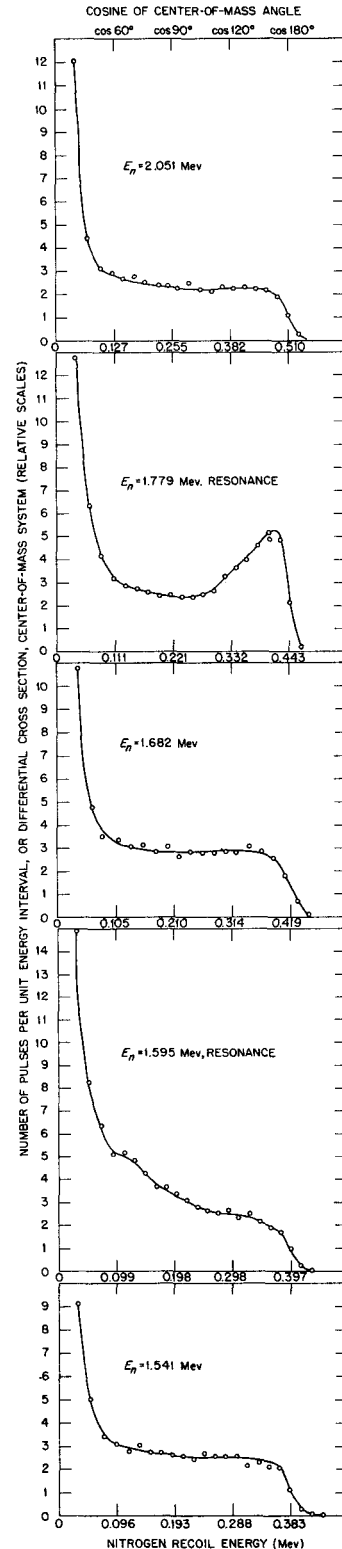


Fig. 1.7. Distribution of Neutrons Elastically Scattered from Nitrogen.

RADIOACTIVITY AND NUCLEAR ISOMERISM

neutrons at the 1.60- and 1.78-Mev resonances. The distributions for neutrons of energy between the resonance energies are also given. It is evident from these curves that the 1.60-Mev resonance corresponds to an increased forward scattering of the neutrons, whereas the 1.78-Mev resonance shows a peak corresponding to backward scatter-

ing of neutrons. The resonance at 1.35 Mev shows a distribution similar to the one at 1.78 Mev. The resonances at 1.40 and at 2.25 Mev are similar to the 1.60-Mev resonance, as far as angular distribution of the scattered neutrons is concerned. The theoretical significance of these distributions is being investigated.

2. RADIOACTIVITY AND NUCLEAR ISOMERISM

COINCIDENCE SPECTROSCOPY OF GAMMA RAYS FROM Ta¹⁸¹

F. K. McGowan

A fast-coincidence spectrometer employing sodium iodide detectors has been developed for both immediate and delayed coincidences. For gamma rays of a few hundred kev, a time resolution of $2\tau = 8.8 \times 10^{-9}$ sec with no loss of coincidences has been realized by using the fast-slow coincidence principle. The trailing edge of a time resolution curve for prompt events has a slope corresponding to a half-period of 5×10^{-10} second. Under these conditions, nuclear metastable states with half-lives $t_{1/2} > 10^{-9}$ sec are measurable.

Some of the *K*-shell internal conversion coefficients of the gamma rays from Ta¹⁸¹ have been remeasured with the faster coincidence spectrometer. In the earlier measurements,⁽¹⁾ the

time resolution was $2\tau = 3.8 \times 10^{-7}$ sec, the new measurements were taken with $2\tau = 1.32 \times 10^{-8}$ second. The improvement in the measurements is realized because it is possible to measure separately the spectrum of the radiation announcing the formation of the 10^{-8} -sec metastable state in Ta¹⁸¹ and the spectrum of the radiation following the decay of the metastable state. The results of the new measurements are tabulated in Table 2.1. Previous measurements of α^K (132 kev) were always somewhat larger because of the sum pulses owing to 132- plus 345-kev gamma rays that could not be distinguished from the 480-kev gamma ray.

The directional angular correlation of the 132- and the 480-kev cascade in Ta¹⁸¹ has been measured as a function

⁽¹⁾F. K. McGowan, *Phys. Quar. Prog. Rep. Dec.* 20, 1951, ORNL-1278, p. 10.

TABLE 2.1. EXPERIMENTAL AND THEORETICAL INTERNAL CONVERSION COEFFICIENTS

NUCLEUS	E_γ (kev)	α_{exp}^K	THEORETICAL COEFFICIENTS*				CLASSIFI- CATION
			α_1^K	α_2^K	α_3^K	β_1^K	
Ta ¹⁸¹	132	0.48 ± 0.02	0.15	0.495		1.94	E2
Ta ¹⁸¹	135	1.88 ± 0.10	0.15	0.495		1.94	M1
Ir ¹⁹¹	128	2.07 ± 0.10		0.518	1.27	3.10	M1 + E2

*M. E. Rose, G. H. Goertzel, B. I. Spinrad, J. Harr, and P. Strong, *Phys. Rev.* **83**, 79 (1951).

RADIOACTIVITY AND NUCLEAR ISOMERISM

of the time of emission of the 480-keV transition. With a liquid source of Hf^{181} metal taken up in 0.025 ml of HF, the anisotropy is independent of the emission time of the 480-keV transition. Measurements have been taken with $2\tau = 1.32 \times 10^{-8}$ and 1.8×10^{-7} second.

Os^{191} TO Ir^{191} DECAY SCHEME

F. K. McGowan

Osmium-191 (15-day) is known to decay by β^- followed by gamma rays of 40 and 128 keV.⁽²⁾ Earlier measurements⁽³⁾ with a scintillation spectrometer employing anthracene detectors indicated that the conversion electrons from the 128-keV transition were not in coincidence with the β^- rays. The measurements have been repeated by using a sodium iodide and anthracene scintillation spectrometer. No coincidences between the β^- rays and the 128-keV gamma radiation were observed. A measurement of the *K*-shell internal conversion coefficient of the 128-keV gamma ray was obtained from the spectrum of the gamma radiation from sources of $\text{Os}^{191,185}$ and Os^{185} (97-day) that is a *K*-capture activity. The value of α^K (128 keV) is tabulated in Table 2.1. From life-time considerations, the transition must be classified *M1* + *E2*, with the intensity ratio of *E2* to *M1* being 0.66. Gamma emission from the 40-keV transition occurs in less than or in 0.5% of the transitions. It is suggested that the 168-keV excited state is metastable.

ANGULAR CORRELATION OF GAMMA RAYS

E. D. Klema F. K. McGowan

The apparatus used in the angular correlation measurements has been extensively modified. A motor is now used to change the position of the movable detector, and data can be

⁽²⁾D. Saxon, *Phys. Rev.* **74**, 1264 (1948).

⁽³⁾F. K. McGowan, *Short-Lived Isomeric States of Nuclei*, ORNL-952, p. 49 (March 13, 1951).

taken automatically in 10- or 45-deg steps from 90 to 270 degrees. A predetermined number of coincidence counts is obtained at each position, and when this occurs, the time of the measurement and the number of single counts in each detector are stamped on paper tapes.

The coincidence circuit has been modified to give greater time stability, with about the same resolving time as that used previously.

The apparatus has also been changed so that the sodium iodide detectors are now irradiated on their flat end surfaces rather than on the curved sides of the cylinders, as was the case previously. This allows the effect of the finite solid angle subtended by the detector at the source to be calculated exactly. Such calculations have been made by the Mathematics Panel, and the correction factors obtained are now being used in the calculation of the data.

Extensive measurements have been made on the angular correlation of the gamma rays emitted by the excited states of Ni^{60} . The proper analysis of the data has been considered in detail. A method has been found for determining the statistical error of each coefficient in the expansion representing the correlation, and the best methods of taking data to minimize the error in the coefficient of the $\cos 4\theta$ term have been investigated. The problem of the proper combination of the data obtained from various runs at a given angle has also been solved.

The data obtained for the Ni^{60} correlation are being analyzed at present in the manner indicated by the considerations just mentioned.

CHEMICAL SEPARATION OF 0.82-sec Pb^{207m} FROM Bi^{207}

E. C. Campbell F. Nelson⁽⁴⁾

It has been presumed that the short-period isomer (half-life 0.82 sec),

⁽⁴⁾Chemistry Division, ORNL.

RADIOACTIVITY AND NUCLEAR ISOMERISM

first found⁽⁵⁾ by fast-neutron irradiation of Pb^{207} , also occurred in the decay of Bi^{207} to Pb^{207} by K -capture. The evidence for this was that two gamma rays at 0.55 and 1.05 Mev found in the Pb^{207m} decay are also found in the Bi^{207} decay.⁽⁶⁾ However, at present there has been no direct proof of the genetic relationship, such as could be obtained by observing the decay of the daughter after chemical separation from the parent.

This experiment has now been performed, which proves directly that the Bi^{207} does decay at least partially via the Pb^{207} isomeric level. The Bi^{207} was produced⁽⁷⁾ by bombarding a lead target with fast protons in the cyclotron, the reaction being $\text{Pb}^{208}(p,2n)\text{Bi}^{207}$. A small portion of the target material was dissolved in nitric acid and then converted to the chloride. Use was made of data obtained by K. Kraus and F. Nelson⁽⁸⁾ on the separation of lead and bismuth with anion-exchange resins (e.g., Dowex-1). They found that in chloride solutions, Bi(III) is considerably more strongly adsorbed than Pb(II) . Thus, almost all the Bi^{207} activity in the sample could be fixed on about 1 cc of the resin in 0.5 N HCl . The lead daughter, being less strongly adsorbed, is expected to diffuse to some extent from the resin into the interstitial solution, from which it could be washed out rapidly. When a few drops of solution were rapidly collected and transferred to a sodium iodide scintillation counter, a short-period activity was immediately evident from the rapid decrease in the observed counting rate.

(5) E. C. Campbell and M. Goodrich, *Phys. Rev.* **78**, 640 (1950).

(6) For additional references and a proposed decay scheme, see M. Goldhaber and R. D. Hill, *Revs. Mod. Phys.* **24**, 179, esp. 231 (1952); M. H. L. Pryce, *Proc. Phys. Soc. (London)* **A65**, 773, esp. 789 (1952).

(7) The authors wish to thank J. A. Martin of the Electromagnetic Research Division, ORNL, for preparing and bombarding the target.

(8) Private communication.

The result definitely establishes the genetic relationship and gives additional chemical support to the proposed decay scheme.⁽⁶⁾ Work is now in progress to use this method for further studies of the daughter activity in a continuous-flow arrangement.

TRITIUM-PRODUCED ACTIVITIES IN NEUTRON-IRRADIATED LITHIUM COMPOUNDS

E. C. Campbell J. E. Strain⁽⁹⁾

When pure lithium fluoride enriched in Li^6 was irradiated in the ORNL graphite reactor, a hitherto unreported activity of 5 ± 1 sec half-life was found, in addition to the well-known 12-sec F^{20} activity. An 0.8-sec activity with radiations identical to those of Li^8 was also obtained, but with an intensity ten times as great as could be accounted for by the reaction $\text{Li}^7(n,\gamma)\text{Li}^8$ on the small residual amount of Li^7 in the sample.

The intensity of the 5-sec activity in lithium fluoride samples of different enrichment is approximately proportional to the amount of Li^6 in the sample; the activity is not found in enriched samples of Li_2SO_4 or in fluorine in a polytetrafluoroethylene sample. It is therefore suggested that the activity is produced by the fast tritons from the $\text{Li}^6(n,\alpha)\text{H}^3$ reaction⁽¹⁰⁾ on the fluorine of the sample. To test this hypothesis, a sample was made that contained enriched Li_2SO_4 sandwiched between thin (1 mg/cm²) strips of polytetrafluoroethylene. When the sample was irradiated, it showed the 5-sec activity, with, however, a much reduced intensity owing to greater dilution of the sample. Of the energetically possible reactions of tritons with fluorine leading to an unstable nucleus, the most likely

(9) Analytical Chemistry Division, ORNL.

(10) E. Almqvist, *Can. J. Research* **28A**, 433 (1950).

NEUTRON DIFFRACTION

seems to be $F^{19}(t,p)F^{21}$. It is proposed to bombard fluorine with tritons in the electrostatic accelerator to settle this point.

The extra intensity of the Li^8 activity found in samples of lithium fluoride enriched in Li^6 is found in both enriched lithium fluoride and enriched Li_2SO_4 . It is proposed that this activity is attributable to another tritium-produced reaction, $Li^6(t,p)Li^8$, studied by Moak, Good, and Kunz⁽¹¹⁾ of this Laboratory, with

(11) C. D. Moak, W. M. Good, and W. E. Kunz, *Phys. Rev.* **85**, 928 (1952).

tritons accelerated in a high-voltage apparatus. Since the Li^6 is at once the source (through tritium production) and the target, it would be expected that the intensity of this activity would depend on the square of relative abundance of Li^6 in the lithium fluoride sample. Also, since Li_2SO_4 is more dilute than lithium fluoride in its lithium content (2/7 vs. 1/2), it would be expected that the intensity of the activity (normalized for equal amounts of Li^6) would be smaller for Li_2SO_4 by the ratio of the dilutions, namely 4/7. Both expectations are verified experimentally within experimental error.

3. NEUTRON DIFFRACTION

NEUTRON-DIFFRACTION STUDIES OF BINARY FERROMAGNETIC ALLOYS

C. G. Shull M. K. Wilkinson

Very little information is available, either theoretically or experimentally, on the values of the atomic magnetic moments that exist in binary alloys of the transition elements. The individual atomic moments certainly must differ from the values that are measurable in the elemental metals, since the magnetic data for the alloys are inconsistent with the pure-element data. For example, the atomic magnetic moments of iron and cobalt are 2.22 and 1.74 Bohr magnetons, respectively, in the pure elements, but in the binary FeCo alloy, the average moment per atom is 2.45 Bohr magnetons. Thus there must exist in the alloy a redistribution of the *d*-shell structure that, in turn, will provide for an altered magnetic moment. Neutron-diffraction measurements should permit an unambiguous determination of the individual moments rather than the average moment per atom that magnetic data supply; hence a study of various alloy systems has been undertaken.

At present, either complete or partial work has been done on three binary combinations: Ni_3Fe , FeCo, and Ni_3Mn . Suitable samples of other groups such as FeCr, Ni_3Cr , NiCo, and CoCr are available and awaiting study or are being prepared.

The study performed on the Ni_3Fe alloy is representative of the procedure and will be described in detail. This alloy can be prepared in either the ordered or the disordered state by proper heat treatment. By prolonged heat treatment at temperatures below the ordering temperature ($T_c = 500^\circ C$), the iron atoms take positions at the corners of the cubic unit cell, and the nickel atoms locate at the face-centered positions of the face-centered cubic structure. In this state, superlattice reflections are observable at the (100), (110), (210), etc. reflection positions in the diffraction pattern, along with the normal (111), (200), and (220) reflections for a face-centered cubic cell. The intensity of the superstructure lines depends upon the difference in scattering power of the two types of atoms and in this case will have two components

NEUTRON DIFFRACTION

caused by (1) a difference in the nuclear scattering amplitudes of iron and nickel, and (2) a difference in the magnetic scattering amplitudes, since the magnetic moments, μ_{Fe} and μ_{Ni} , differ. By measuring the latter, evaluation of the individual moments is possible. In contrast to the ordered state, disordered samples in which there is a random distribution of iron and nickel atoms at face-centered cubic positions can be produced by quenching the alloy from a temperature well above the ordering temperature or by severely cold-working the material, such as by filing. If the magnetic moments of iron and nickel differ in such a disordered lattice, there should exist in the diffuse scattering a ferromagnetic disorder scattering that is proportional to the difference between the moments. This scattering is similar to the normal isotopic disorder scattering and is recognizable by its magnetic form-factor variation and its sensitivity to an applied external magnetic field.

The magnetic portion of the superstructure lines in the ordered samples can be determined in two independent ways: (1) The observed intensity can be corrected for nuclear superstructure contribution and for higher order neutron wave-length contribution⁽¹⁾ and the residue ascribed to magnetic scattering; and (2) the superstructure intensity can be studied with a magnetized sample in which the magnetic scattering is affected in a known fashion, thereby permitting its evaluation. Both methods have been used advantageously for the case of ordered Ni_3Fe ; the results are summarized in Fig. 3.1. The magnetic portion of four superlattice reflections expressed in absolute units of differ-

(1) The monochromating crystal in the spectrometer reflects a small amount of $\lambda/2$, $\lambda/3$, etc., components of known intensity in addition to the primary wave length.

ential scattering cross section is shown as a function of the scattering angle variable $\sin \theta/\lambda$. Data obtained by the two methods agree surprisingly well, and the magnetic intensity is seen to follow a normal magnetic form-factor dependence on scattering angle. The curve drawn through the points is the theoretical form-factor curve for metallic iron, as calculated by Steinberger and Wick, and the intercept value at small angles is taken as 0.220×10^{-24} cm² per Ni_3Fe molecule. This value permits determination of the difference ($\mu_{Fe} - \mu_{Ni}$) between the two magnetic moments according to

$$F^2(\text{magnetic superstructure}) = 0.0484 \times 10^{-24} (\mu_{Fe} - \mu_{Ni})^2$$

Thus $(\mu_{Fe} - \mu_{Ni}) = 2.11$ Bohr magnetons. The individual moments can be calculated by combining this result with the saturation magnetization data for this alloy, which provides a different linear combination of the individual moments. Thus magnetic studies yield

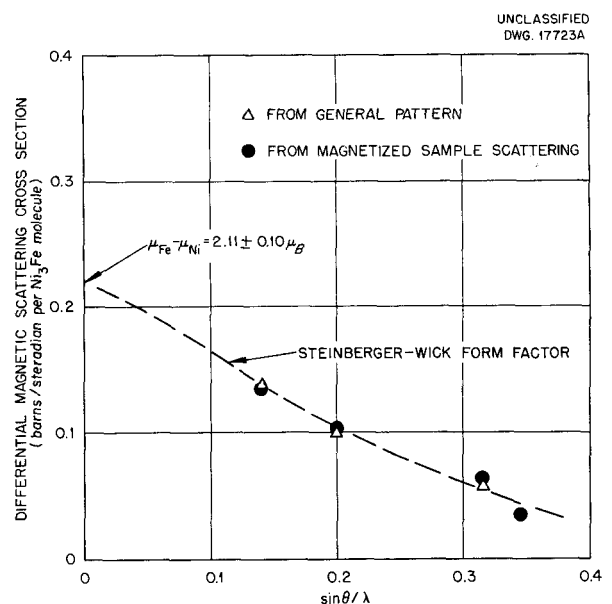


Fig. 3.1. Superstructure Lines in Ordered Ni_3Fe .

NEUTRON DIFFRACTION

a magnetic moment of 1.21 Bohr magnetons per average atom and hence

$$\frac{3}{4} \mu_{\text{Ni}} + \frac{1}{4} \mu_{\text{Fe}} = 1.21 .$$

Combination of the two equations yields two sets of solutions: $\mu_{\text{Fe}} = +2.79$ and $\mu_{\text{Ni}} = +0.67$, or $\mu_{\text{Fe}} = -0.4$ and $\mu_{\text{Ni}} = +1.7$. The second set of values can probably be ruled out, since it represents a drastic change from the pure-element values.

For the disordered alloy, a difference between the iron and nickel magnetic moments will result in the appearance of a magnetic disorder scattering that will be superimposed on the various other components of the diffuse scattering in the pattern. Because of the low intensity of this magnetic disorder scattering, it is difficult to establish its presence in the general pattern, but it can be seen as a change in intensity when the sample is magnetized. Figure 3.2 shows the observed change in intensity of the diffuse scattering upon magnetization when this change is placed on an absolute scale where it is seen to follow the expected form-factor dependence with angle. The extrapolated value for the cross section at zero angle again yields the difference between the iron and nickel moments, and this difference is evaluated as $2.0 \mu_B$. Within experimental error, this value is the same as that obtained for the ordered sample and

suggests that the individual atomic moments are independent of the state of order or disorder in the lattice.

Similar studies have been made on ordered samples of FeCo and Ni_3Mn , and the magnetic moments of the individual atoms have been determined. The moments thus determined are summarized in Table 3.1. It is to be noted that the iron moment as determined in both FeCo and Ni_3Fe averages about 2.8 Bohr magnetons and that this is significantly higher than the normal moment of 2.22 magnetons found in elemental iron. On the other hand, the nickel and cobalt moments in these alloys do not appear to be significantly different from their elemental values of 0.60 and 1.74 magnetons, respectively. It is of interest that the difference between the two moments in the individual binary alloys is approximately the same as the difference between the atomic numbers.

MAGNETIC SCATTERING OF NEUTRONS BY NEODYMIUM AND ERBIUM

W. C. Koehler E. O. Wollan

Results have been given in previous quarterly reports on the paramagnetic scattering of neutrons by trivalent ions in rare-earth oxides. The measurements were made at temperatures as low as the temperature of liquid hydrogen, and no appreciable change in the character of the magnetic scattering was observed.

A study has also been made of the magnetic scattering by the metals, neodymium and erbium, that have been made available through the courtesy of F. A. Spedding of Iowa State College, Ames, Iowa.

Neodymium metal was found to behave similarly to the trivalent ions in the oxides, the magnetic scattering being of the paramagnetic type at temperatures as low as the temperature of liquid helium.

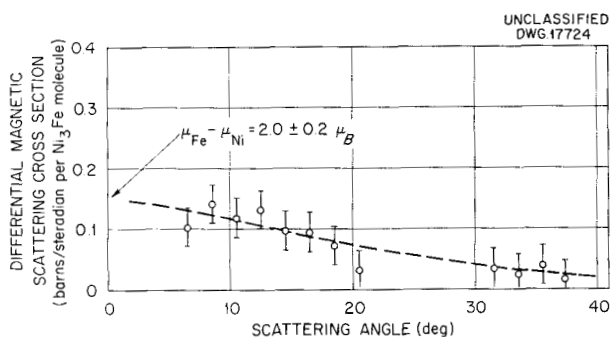


Fig. 3.2. Ferromagnetic Disorder Scattering in Disordered Ni_3Fe .

NEUTRON DIFFRACTION

TABLE 3.1. MAGNETIC MOMENTS IN FERROMAGNETIC ALLOYS

ALLOY	MAGNETIC MOMENT OF CONSTITUENTS	
Ni ₃ Fe		
Ordered	$\mu_{Fe} = 2.8 \pm 0.2 \mu_B$	$\mu_{Ni} = 0.7 \pm 0.1 \mu_B$
Disordered	$\mu_{Fe} = 2.7 \pm 0.2 \mu_B$	$\mu_{Ni} = 0.7 \pm 0.1 \mu_B$
FeCo		
Ordered	$\mu_{Fe} = 2.9 \pm 0.2 \mu_B$	$\mu_{Co} = 1.9 \pm 0.2 \mu_B$
Ni ₃ Mn		
Ordered	$\mu_{Mn} = 2.9 \pm 0.2 \mu_B$	$\mu_{Ni} = 0.4 \pm 0.1 \mu_B$

Erbium metal, on the other hand, had been predicted from resistance measurements to be ferromagnetic below the temperature of liquid nitrogen, and the neutron measurements bear out these predictions. Erbium has been studied over the temperature range from 77 to 4°K, and its ferromagnetic properties have been found to be somewhat complex. In the range from 20 to 4°K, there appears to be a transition in which the moments line up along the *c*-axis of the hexagonal close-packed arrangement, which is the known stable form for these metals. In the range from somewhere above the temperature of liquid nitrogen to about 20°K, the coherent magnetic scattering gives an entirely different diffraction pattern, the interpretation of which has not yet been accomplished.

The data and interpretation will be discussed in detail in a future report.

It can be stated at this time, however, that the observed coherent magnetic scattering has a large angular momentum contribution, the effective magnetic moment being near that for the free ion ($\mu_{eff} = 9.5$ Bohr magnetons). The further study of ferromagnetism in the rare earths in which the 4-*f* electrons that are responsible for the magnetism are deeply buried in the atom, should be of importance in the better understanding of the general nature of exchange coupling.

The fact that the moments lie along a fixed axis (the *c*-axis) at low temperatures will permit a study to be made of the angular dependence of the 4-*f* electronic wave functions in the solid.

NEUTRON CROSS SECTIONS AND NEUTRON DECAY

4. NEUTRON CROSS SECTIONS AND NEUTRON DECAY

TIME-OF-FLIGHT SPECTROMETER STUDIES

G. S. Pawlicki E. C. Smith
P. E. F. Thurlow

Measurements with the time-of-flight spectrometer have been made on normal nickel and on a sample enriched in Ni^{62} by using a resolution of $0.50 \mu\text{sec}/\text{meter}$.

Nickel. The results on normal nickel are shown in Fig. 4.1. Spectrographic analysis of the sample showed 0.018% iron, less than 0.005% manganese, and less than 0.003% cobalt. The transmission dip at 120 ev is probably due to cobalt impurity.

Nickel-62. The mass analysis supplied with the sample of Ni^{62} showed the following composition: Ni^{58} , 3.4%; Ni^{60} , 3.1%; Ni^{61} , 0.3%; Ni^{62} , 92.7%; Ni^{64} , 0.5%. A strong resonance is

evident at 4200 ev, as shown in Fig. 4.2. The area under the transmission dip shows that this level has a "strength," $\sigma_0 \Gamma^2 = 1.1 \pm 0.1 \times 10^9$ barn-ev². If, as might be expected, the resonance is due primarily to S-wave scattering, $\sigma_0 = 4\pi\lambda_0^2 = 620$ barns, then $\Gamma = 1300$ ev.

NEUTRON DECAY

F. Pleasonton H. L. Reynolds
A. H. Snell

Inconclusive results were obtained in an attempt to measure the momentum spectrum of the protons recoiling as a result of beta emission from neutrons. A beam of neutrons about 1 in. in diameter was taken from the LITR, and a magnetic lens was arranged at right angles to gather particles from a

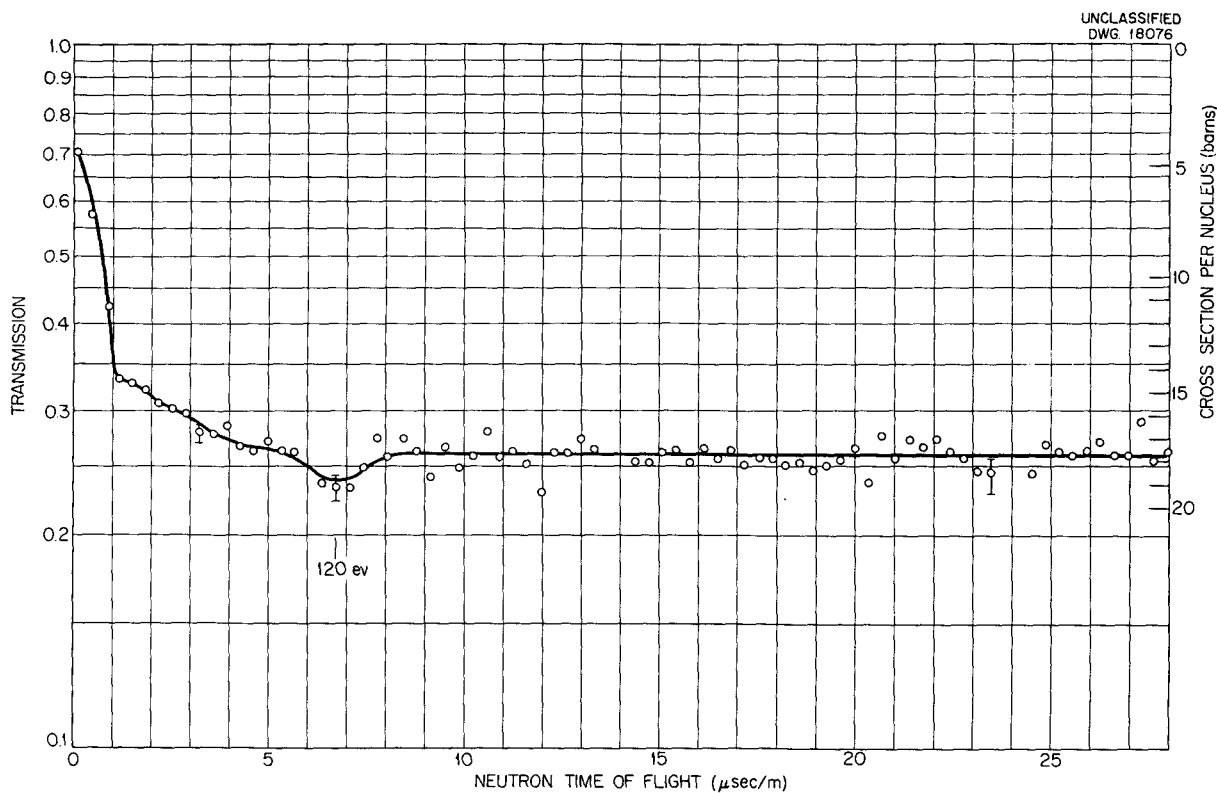


Fig. 4.1. Transmission of Nickel Obtained by Using a $7.52 \text{ g}/\text{cm}^2$ Sample.

NEUTRON CROSS SECTIONS AND NEUTRON DECAY

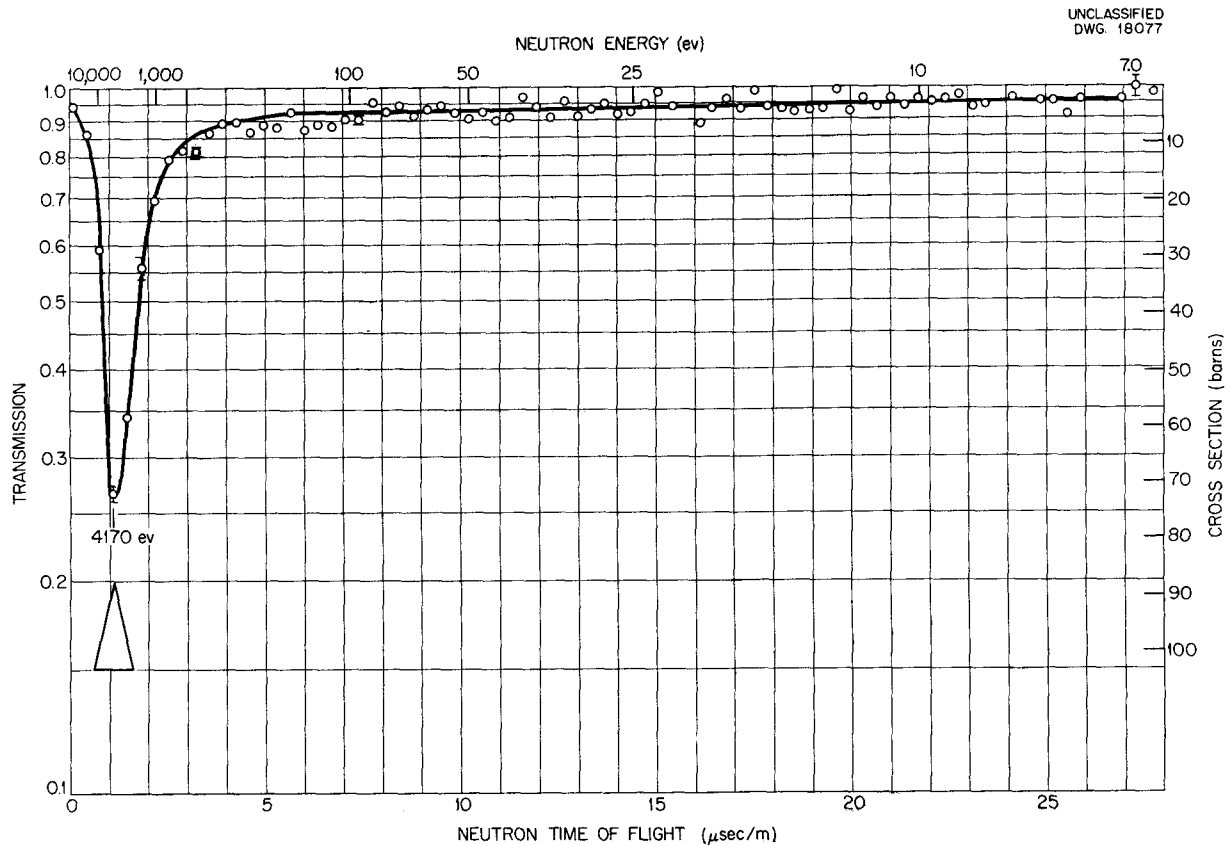


Fig. 4.2. Transmission of Ni⁶² Obtained by Using a 1.89 g/cm² Sample.

short section of the beam. Recoiling protons were to drift through the lens, and at the focal position they were to be accelerated onto a multiplier for counting. Variation of the lens current would enable the spectrum to be run under conditions of low resolution. At best, only a low counting rate was to be expected. Actually, a few counts per minute were found that behaved as they should if they originated in neutron decay, but they appeared to be so entangled with other effects arising from ionization of the residual gas in the vacuum system that it was impossible to have sufficient confidence in the identification of the effect. The work was abandoned when a more promising approach occurred.

Consider an evacuated, conical vessel in the thermal column of the MTR (Fig. 4.3). Such a vessel might

be 2 meters long, and with a 4-deg half-angle of taper, it would have a volume of 20 liters or more. Neutrons would decay in this volume, and some of the recoiling protons would emerge in a collimated beam from the hole at the narrow end, after which they would be deflected by a double-focusing magnet. An appropriate electric deflection following the magnetic deflection would, by mass-spectrometer action, select only particles of mass 1. Postdeflection acceleration would be applied in order to count the protons by means of a multiplier. Such a geometry is much more favorable for proton collection than was that of the LITR experiment described in the previous paragraph, because only one solid-angle loss is incurred instead of two. Furthermore, it might lend itself to a half-life determination

NEUTRON CROSS SECTIONS AND NEUTRON DECAY

UNCLASSIFIED
DWG. 18078

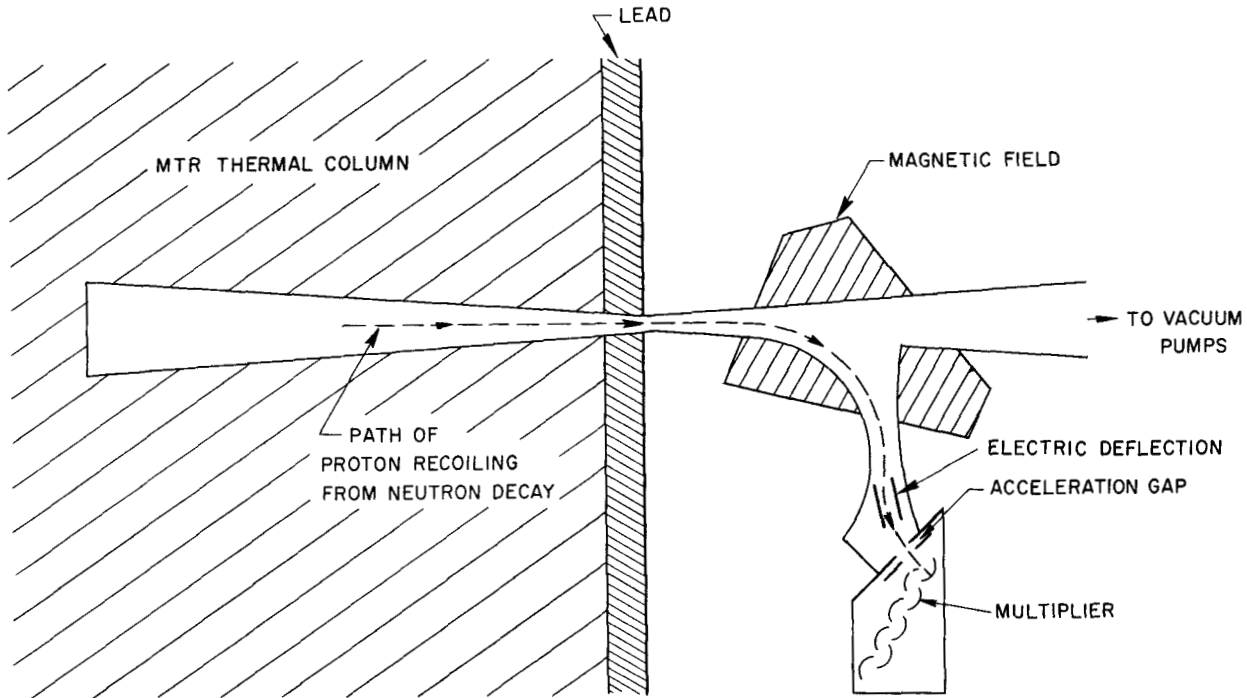


Fig. 4.3. Proposed Experiment for Recoil Momentum Measurement.

provided only that the transmission through the deflection system could be accurately evaluated.

Some study was devoted to a consideration of perturbing effects in such an experiment. Scattering of fast neutrons in the hydrogen of the residual gas would not be serious. Recoiling protons from hydrogen in or on the walls would cause more concern and would necessitate outgassing. Although the thermal $N^{14}(n,p)C^{14}$ reaction might be expected to give trouble, it need not because (1) it is exothermic and (2) a nitrogen-free metal can be selected for the wall material. Neutralization of the protons along their paths would be negligible. The most conceivable dangerous effect is the recoiling of protons in the residual gas as a result of electron scattering. The high gamma-radiation field present in the MTR thermal column will provide many high-speed electrons,

and the limit to the amount of hydrogen permissible in the conical source-volume becomes very low. However, with outgassing and with the use of mercury diffusion pumps, this limit might be attainable.

The experiment is believed to be worthy of further study, but as a preliminary it will be tried with He^6 instead of with neutrons. The He^6 can be generated in a reactor or cyclotron and then piped into the conical source volume. From this point, the experiment is the same, with the exception that He^6 is much more favorable intensity-wise, and the experiment can be done in Oak Ridge. From the point of view of beta-decay theory, He^6 is as important as neutron decay.

A magnet and a power supply have been found; equipment has been designed, and some of it has been received from the machine shop.

5. HEAVY-ION PHYSICS

EQUIPMENT AND TECHNIQUES

G. E. Evans P. M. Stier
C. F. Barnett V. L. DiRito

During the last six months, the major effort of the Heavy-Ion Physics group has been devoted to rebuilding the experimental facilities in the new quarters in Building 5500. A new Cockcroft-Walton type of power supply capable of producing 250 kv at 5 ma was purchased from Beta Electric Co. and has been placed in operation with a rebuilt accelerator tube and vacuum equipment. Experiments have been initiated to determine the mean charge of ions (number of electronic charge units per number of particles in the beam) in a heavy-ion beam after it was passed through a thin gas target at various energies. No numerical results are yet available from this program.

In a previous quarterly report,⁽¹⁾ results were given from experiments on the distribution in space of ionization produced by a collimated beam of heavy ions entering a gas target. By using this notation,⁽¹⁾ consideration can be given to the ionization current produced in a very small (approximately 1 mm³ volume) ionization chamber located at a point (R, r) in space, where R is the axial and r the radial distance of the ionization chamber from the entrance pinhole at $(0, 0)$. If, in a given region in space, the number of ions produced per unit volume per time is defined as n , then the current produced in an ionization chamber placed within this region should be proportional to the volume of the ionization chamber, provided only that n varies uniformly in this region (dn/dR and dn/dr are nearly constant) and that the ionization

chamber is operated at an appropriate voltage to obtain saturation of the current. It is evident that this condition is not met at points close to $(0, 0)$. In particular, at the point $(0, 0)$ itself, the ionization current varies nearly linearly with the thickness of the ionization chamber but is almost independent of the ionization chamber diameter, provided that the diameter is larger than that of the entrance pinhole (as was the case in the experiments just mentioned). All the ionization chambers used in these experiments have been very thin, so that attenuation of the ionization within the thickness of the chamber itself can be ignored.

In the preceding presentation of data,⁽¹⁾ it was stated, without demonstration, that it is possible to compute from results obtained at one gas pressure what the distribution of ionization density should be at any other arbitrary pressure. As an afterthought, it now appears appropriate to demonstrate the method by means of which this transformation is accomplished, since it is not self-evident.

Assume that the ionization current produced in a small ionization chamber is i'_1 at the point (R_1, r_1) in a gas at pressure P_1 . Let the current produced in the same ionization chamber at the point $(0, 0)$ at the same pressure and initial beam be i_1 . Define C_1 as $100 i'_1/i_1 v$, where v is the ionization chamber volume. Assume now that the pressure is changed to a new value P_2 and that the ionization chamber is shifted to the position (R_2, r_2) , where $R_2 = R_1 P_1/P_2$ and $r_2 = r_1 P_1/P_2$. Let the ionization chamber currents at (R_2, r_2) and $(0, 0)$ be i'_2 and i_2 , respectively, which give

$$C_2 = 100 \frac{i'_2}{i_2 v} .$$

⁽¹⁾G. E. Evans, P. M. Stier, C. F. Barnett, and V. L. DiRito, *Phys. Quar. Prog. Rep. March 20, 1952, ORNL-1289, p. 20.*

HEAVY-ION PHYSICS

Consider first the relation i_1 to i_2 . The ionization chamber used is larger than the diameter of the entrance pinhole, so that at the position (0,0) all the ion beam enters the ionization chamber, whether the pressure is P_1 or P_2 . However, the change in pressure from P_1 to P_2 changes the density of gas in the ionization chamber by a factor P_1/P_2 , so that under the conditions of the experiment $i_1/i_2 = P_1/P_2$.

The relationship between i_1' and i_2' may be found similarly. By assuming that the positions (R_1, r_1) and (R_2, r_2) are both far enough from (0,0) that the ionization density varies slowly and uniformly over the volume of the ionization chamber, then $i_1'/i_2' = P_1^3/P_2^3$. The right side of this equation may be considered the product of two factors: a factor P_1/P_2 arising from the change in density of gas in the ionization chamber with pressure; and a factor P_1^2/P_2^2 arising from the change in the number of ions entering the ionization chamber. Notice that the contours defined by the ionization density C_1 and C_2 are similar figures and that the points (R_1, r_1) and (R_2, r_2) are corresponding points on these similar figures. An increase in pressure from P_1 to P_2 may be considered to "shrink" the ionization density contours to a smaller size. When the ionization chamber is placed on the shrunken contour at pressure P_2 , the ionization current is not i_1' but a larger value $i_1' P_2^3/P_1^3$, since the ionization chamber now intercepts a larger fraction of the total flux of ionizing particles.

By combining these results, the equation $C_1/C_2 = P_1^2/P_2^2$ is obtained.⁽¹⁾ This equation has been checked experimentally for He^+ ions in helium gas, He^+ ions in argon gas, A^+ ions in helium gas, and A^+ ions in argon gas and is found to be valid to within less than 5%. By knowing that the locus (R_1, r_1) of points at pressure P_1 for C is some known value C_1 , it is possible to compute from the equation

the locus (R_2, r_2) for any other pressure P_2 , where the corresponding value of ionization density is given by $C_2 = C_1 P_2^2/P_1^2$.

Several interesting properties of the ionization density contour may be derived from the foregoing considerations. Let V_1 be the volume of the contour at pressure P_1 for which $C = C_1$, and V_2 be the volume of the contour at pressure P_2 for which $C = C_2$. The contour curves corresponding to the values C_1 and C_2 are similar figures, and thus their volumes are in the ratio of the cube of a suitable linear dimension. Since, as derived above, the coordinates of any point (R_2, r_2) on contour C_2 are related to points on the contour C_1 by relations of the type $R_2 = R_1 P_1/P_2$ and $r_2 = r_1 P_1/P_2$, it follows that the volume of the contours C_1 and C_2 vary as the cube of the pressure: $V_1/V_2 = P_2^3/P_1^3$. Since $P_2/P_1 = C_2/C_1$, it may be written that $V_1/V_2 = P_2^3 C_2/P_1^3 C_1$; $C_2/C_1 = P_1^3 V_1/P_2^3 V_2$.

From these relationships, it is seen that contours with the same value of C contain equal numbers of atoms (from $PV = nRT$, where T is constant).

The characteristics of an Allen-type electron multiplier have been investigated to determine the feasibility of its use in the quantitative detection of low-energy positive ions. The multiplier consists of 12 dynodes with an operating voltage of 470 volts per stage. Incident ion current to the multiplier is measured with a Faraday cup connected to a balanced bridge electrometer. After an initial decrease in gain of 30% during the first 2 hr of operation, the gain has been found to be approximately 10^5 . At later times, no noticeable decrease has been observed.

Some of the characteristics of the multiplier are shown in Figs. 5.1 through 5.4. In Fig. 5.1, it is seen that the gain increases with particle

HEAVY-ION PHYSICS

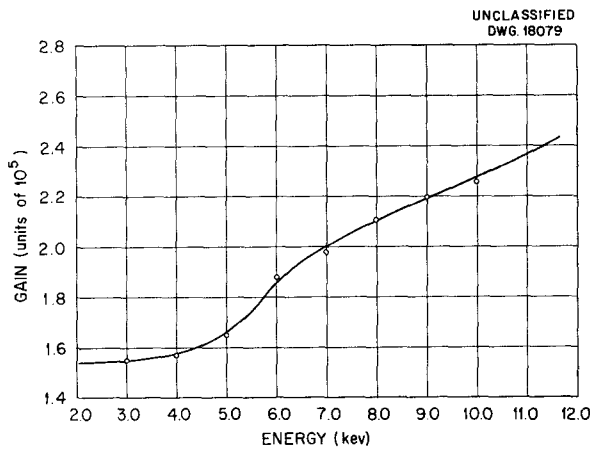


Fig. 5.1. Gain vs. Particle Energy.

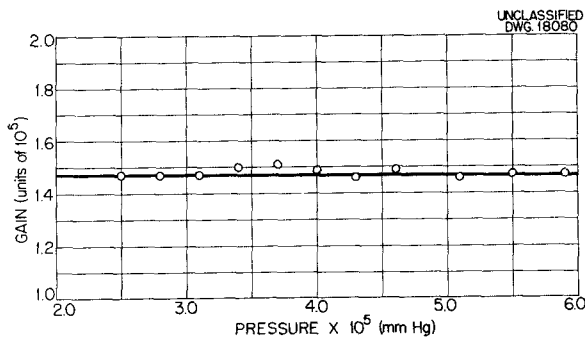


Fig. 5.2. Gain vs. Pressure.

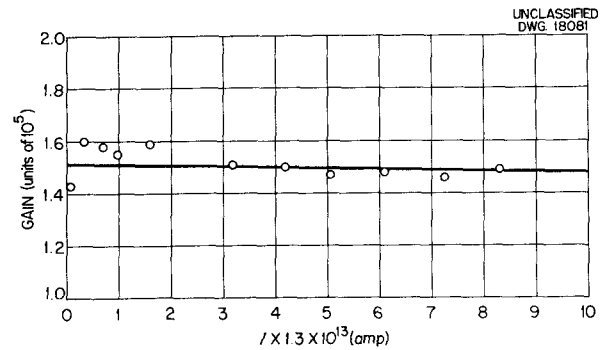


Fig. 5.3. Gain vs. Input Current.

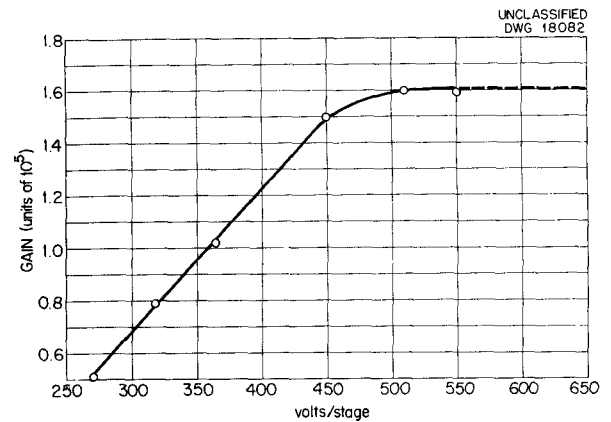


Fig. 5.4. Gain vs. Multiplier Voltage.

(H_2^+) energy in the range of 3 to 10 kev. Figures 5.2 and 5.3 show the stability of the gain when the pressure or input current is varied. The slight rise of gain in Fig. 5.3 at low ion currents probably results from the uncertainty of measuring the current. Figure 5.4 shows a saturation of gain at approximately 450 volts per stage. The gain for H_2^+ is approximately 30% greater than that for H^+ for the same energy. Equipment changes are being

made to provide more consistent data for the higher masses.

Alpha particles from Po^{208} have been counted successfully. Background count is from 5 to 20 cpm. Pulse heights from the electron multiplier range from 0.25 to 2.5 mv. Use of the alpha source with present geometry allows only a rough estimate of the efficiency, which is approximately 80 to 100%.

6. THEORETICAL PHYSICS

PRODUCTION OF POLARIZED PARTICLES
IN NUCLEAR REACTIONS

A. Simon T. A. Welton

Schwinger⁽¹⁾ has shown that polarized neutrons may be obtained by the elastic scattering of neutrons from He⁴. This result, however, is seen to be a special case of a more general theorem that, under suitable conditions, the products of any nuclear reaction will be polarized. As a result, it should be possible to use resonant charged-particle reactions to obtain directly (rather than by an intervening elastic scattering) high-intensity beams of polarized neutrons with energies variable over a considerable range.

A general expression for the polarization resulting from nuclear reactions has been obtained. The sums over magnetic quantum numbers, which are essentially geometrical in nature, have been performed; the results are given in terms of Racah functions.⁽²⁾ The following general results have been obtained:

1. The polarization is always perpendicular to the plane formed by the directions of the incident and emitted particle.

2. If only S-waves are effective in the reaction, for either the incident or the final states, there can be no polarization.

3. If only levels of the compound nucleus having $J = 1/2$ (or 0) and a single parity are effective, there will be no polarization.

4. Polarization results from the interference of different subchannels (i.e., partial waves or final channel spins) contributing to the reaction. (The state of the residual nucleus must always be the same, of course.) Hence, if there is only a single

incident subchannel leading to a single level and breaking up into a single final subchannel, the polarization will vanish.

5. If there is no spin-orbit coupling, the polarization is zero.

The final result yields the following expression for the dependence of the intensity of polarization upon the angle between the incident and emitted beam:

$$P = \sum_{L=1}^{\infty} A_L P_L^1(\cos \theta), \quad (1)$$

where P_L^1 is the associate Legendre function, and A_L is a complicated expression involving several Racah functions and the scattering matrix for the reaction. The results have a formal similarity to the expression previously obtained for the angular dependence of reaction cross sections.⁽³⁾ In particular, if there is a largest effective incident orbital partial wave, l_{\max} , or a largest final wave, \bar{l}_{\max} , or a largest spin, J_{\max} , of the compound nucleus, then the largest value of L in Eq. 1 is given by the simultaneous conditions

$$L \leq 2l_{\max}, \quad L \leq 2\bar{l}_{\max}, \quad L \leq 2J_{\max}. \quad (2)$$

These rules are identical to the rules for the limitation of the complexity of angular distributions⁽⁴⁾ and follow from the requirements for the nonvanishing of the Racah coefficients.

It is interesting to note that even a single level of definite J ($\neq 1/2$ or 0) and parity will produce polarization if more than one subchannel (l -value or final channel spin) contributes. Several known reactions offer promise. In particular,

(1) J. Schwinger, *Phys. Rev.* **69**, 681 (1946).

(2) G. Racah, *Phys. Rev.* **62**, 438 (1942).

(3) J. M. Blatt and L. C. Biedenharn, *Phys. Rev.* **82**, 123 (1951).

(4) C. N. Yang, *Phys. Rev.* **74**, 764 (1948).

analyses⁽⁵⁾ of the angular distributions of (p, n) neutrons resulting from resonances in C^{13} , B^{11} , Li^7 , and H^3 indicate that P -waves, or higher, and opposite parities are interfering. It seems likely that many neutron sources, hitherto considered unpolarized, may actually exhibit partial polarization.

A letter on the subject has been submitted to the *Physical Review*. Details of the calculations will appear in a paper to be submitted to the same journal in the near future.

QUANTUM ELECTRODYNAMICS

T. A. Welton

A systematic calculation of the level shift in hydrogen by using the general methods described in previous quarterlies is in progress. The aim is to provide a sufficiently precise calculation of the electrodynamic part of the level shift to enable the decision to be made (by comparison with the existing experimental results) as to whether the positron contributions to the level shift should be included. The best existing calculations seem to require very strongly that the positron effects be included.

The calculation is not yet complete, but has been carried to the point where two clear (and important) effects have been found, which seem to have been omitted in previous calculations.

$$m\psi = \gamma^\mu p_\mu \psi + \gamma^\mu V_\mu \psi + \frac{1}{2} e [iS, \gamma^\mu A_\mu] \psi + [iS, \gamma^\mu V_\mu] \psi + \frac{1}{2} [iS, [iS, \gamma^\mu V_\mu]] \psi, \quad (2)$$

A third effect in this category has been partially demonstrated, but its

⁽⁵⁾H. B. Willard, private communication.

calculation is more difficult; therefore it is not anticipated that the precision of the final result will equal that of Lamb's experiment. It is hoped, however, that the evidence for the inadequacy (if any) of previous calculations can be made sufficiently strong to allow a reopening of the whole question.

A convenient starting point is the wave equation for the electron in the hydrogen atom (interacting also with the electromagnetic field):

$$m\psi = \gamma^\mu p_\mu \psi + \gamma^\mu V_\mu \psi + e\gamma^\mu A_\mu \psi, \quad (1)$$

where the notation is essentially uniform with that given in previous quarterlies. Here, however, V_μ is the external four-potential energy acting on the electron (in this case V_0 is the potential energy due to the proton and $V_1 = V_2 = V_3 = 0$). The symbol A_μ refers to the quantized electromagnetic four-potential, for which an expression was previously given. The problem is to determine the change in the parameter m that is required to hold the energy of a given atomic state constant as the coupling constant e is changed from zero to its actual value.

It is convenient to introduce a contact transformation designed to yield an explicit solution of the problem to order e^2 , if V_μ were to vanish. The generating function, S , for this transformation is easily found, and Eq. 1 transforms to

correct to terms in e^2 , remembering that S is of order e .

The required mass change for the zeroth unperturbed state is given by

$$\delta m_0 = \frac{e}{2} (0 | [iS, \gamma^\mu A_\mu] | 0) + \frac{1}{2} (0 | [iS, [iS, \gamma^\mu V_\mu]] | 0) + (0 | [iS, \gamma^\mu V_\mu] (m_0 - \gamma^\mu p_\mu - \gamma^\mu V_\mu)^{-1} [iS, \gamma^\mu V_\mu] | 0), \quad (3)$$

THEORETICAL PHYSICS

again correct to order e^2 , which is easily shown to be adequate for this purpose. The notation indicates that expectation values of the operators are to be taken for the unperturbed state, and the bar above refers to the vacuum average that must be performed in order to obtain a numerical result.

The first term in Eq. 3 is actually infinite, and for a free particle it yields the usual diverging integral for the mass correction. If the mass correction (δm) for a free particle at rest is subtracted, the remainder is finite and observable.

The resulting level shift is then given by

$$\delta E_0 = (0|\delta M - \delta m|0) + (0|\delta V|0) + (0|Q|0) + (0|R|0), \quad (4)$$

$$\delta M \equiv \frac{e}{2} [iS, \gamma^\mu A_\mu],$$

where expectation values in the usual sense (elementary Dirac single-particle theory) are now indicated. The last term is commonly called the second-order level shift. It can be approximately evaluated by reference to existing work, and no improvement of this term is attempted here. The second term can also be evaluated by reference to previous work, which exhibits the operator δV as a simple integral operation on the potential energy function V . Both the first term and the third term (which combine to give a convergent contribution) have apparently been ignored previously. Their contribution can be shown to be proportional to the expectation value of an operator that is essentially p^2 (or an operator that is equivalent nonrelativistically).

The following qualitative conclusions can now be given:

1. The first and third term, although they cannot contribute to the line shift (difference of level shifts for $2S_{1/2}$ and $2P_{1/2}$ states) in the lowest order, will actually give a line shift in the order $\alpha^5 m$ (which is

the order of the main level shift) because of relativistic effects.

2. The second term is customarily evaluated by taking the hydrogen wave functions to be constant in the neighborhood of the proton. This procedure is actually in error by an amount of order α times the main level shift, because the function δV has a finite range of order $1/m$. A simple calculation indicates that the level shift should be reduced by about 10 megacycles/sec.

3. The second-order shift (term four) apparently contains an error of order $\alpha^5 m$, for the $2S_{1/2}$ state, but its correction involves a prohibitive amount of labor - prohibitive, at least, until the necessity is clearly indicated by the numerical results for Eqs. 1 and 2.

MAGNETIC SCATTERING OF SLOW NEUTRONS BY ATOMS WITH NONZERO ORBITAL ANGULAR MOMENTUM

G. T. Trammell

The methods described in the previous quarterly⁽⁶⁾ for calculating the scattering of slow neutrons by atoms with orbital moments have been extended. Calculations are in progress that should yield predictions of the scattering from rare-earth atoms over a range of energy and angle that was previously inaccessible.

EFFECT OF FINITE DeBROGLIE WAVE LENGTH IN BETA DECAY

M. E. Rose

In the theory of beta decay, the energy distribution for both allowed and forbidden transitions depends on the values of various electron (or positron) wave functions evaluated at the nuclear radius. In the notations of Greuling⁽⁷⁾ and Pursey,⁽⁸⁾ the

⁽⁶⁾G. T. Trammell, *Phys. Quar. Prog. Rep.* Sept. 20, 1952, ORNL-1415, p. 19.

⁽⁷⁾E. Greuling, *Phys. Rev.* **61**, 568 (1942).

⁽⁸⁾D. L. Pursey, *Phil. Mag.* **42**, 1193 (1951).

quantities depending on these wave functions were L_ν , M_ν , N_ν (for pure interactions) and, in addition, P_ν , Q_ν , R_ν enter for mixed interactions. These quantities are functions of p , the electron (positron) momentum, and of Z . The index ν that has the range 0 through n for n th forbidden transitions is related to the beta particle angular momentum J , by $\nu = J - 1/2$. It has been customary to evaluate the six functions mentioned above for given ν by replacing the confluent hypergeometric series, which enters in the wave functions⁽⁹⁾ by the first or first two terms. In fact, without the use of high-speed computing machines, no other procedure is practical.

The approximation involved in this procedure has always been regarded as a good one. However, just how good it is cannot be seen so easily without resort to an essentially exact calculation that would evaluate the series to a high degree of precision. It was noted that in some cases the approximate formula gave results that were far from correct (wrong sign of M_ν for positrons and $p \sim 10$, units mc). In view of this fact, a computational program was set up to evaluate these functions in an essentially exact manner. This was done not only for the reason cited but also because the approximate formulas for forbidden transitions were sufficiently complicated to require that rather elaborate numerical work be done in order to provide tables for easy analysis of any forbidden transition. The exact calculations were not much more formidable than the approximate ones.

The results were that for most cases the values of the wave function combinations given by the approximate

formulas (which were also computed) were quite satisfactory. However, the following exceptions were noted:

1. The values of M_ν , now of the correct sign, deviated from the approximate values for $p \sim 9$. This is a rather high energy, however.

2. The values of L_0 deviated from the approximate L_0 (the latter being energy independent and the same for electrons as for positrons). The correct L_0 showed a deviation that increased with Z , of course, and a modification of the spectrum that is most important for larger maximum energies. Without entering into further detail at this point,⁽¹⁰⁾ it will suffice to say that the resultant curvature in a Fermi-Kurie plot is important enough to require that this effect be taken into account wherever $Z > 40$ and for $W_0 \gtrsim 5$. These limits are somewhat arbitrary, and with increased experimental precision they would be lowered (see next paragraph).

3. Modifications in forbidden spectra with unique matrix elements were examined. Here, as in the case of the allowed spectra, an appreciable correction factor is introduced. However, for those measured spectra where Z and W_0 are not small, only a portion of the spectrum could be expected to give a linear plot owing to source and backing distortion. In some cases, replotting the data yields a new straight line (as judged by the eye) but with a smaller slope. Of the existing data, it can be said that no errors of interpretation could occur. This is especially true where the data are not so precise.

⁽¹⁰⁾ For numerical results, see M. E. Rose, C. L. Perry, and N. M. Dismuke, *Tables for the Analysis of Allowed and Forbidden Beta Transitions*, ORNL-1459 (Feb. 11, 1953). A discussion of the results appears in a paper (M. E. Rose and C. L. Perry) submitted to the *Physical Review*.

⁽⁹⁾ M. E. Rose, *Phys. Rev.* **51**, 484 (1937).